# Generation of helical magnetic field in a viable scenario of inflationary magnetogenesis

Ramkishor Sharma,[1,*] Kandaswamy Subramanian,[2,†] and T. R. Seshadri[1,‡]

[1]Department of Physics and Astrophysics, University of Delhi, New Delhi–110007, India
[2]IUCAA, Post Bag 4, Pune University Campus, Ganeshkhind, Pune–411007, India

(Received 13 February 2018; published 4 April 2018)

We study the generation of helical magnetic fields in a model of inflationary magnetogenesis which is free from the strong coupling and backreaction problems. To generate helical magnetic fields, we add an $f^2\tilde{F}^{\mu\nu}F_{\mu\nu}$ term to the Lagrangian of the Ratra model. The strong coupling and backreaction problems are avoided if we take a particular behavior of coupling function $f$, in which $f$ increases during inflation and decreases postinflation to reheating. The generated magnetic field is fully helical and has a blue spectrum, $d\rho_B/d\ln k \propto k^4$. This spectrum is obtained when coupling function $f \propto a^2$ during inflation. The scale of reheating in our model has to be lower than 4000 GeV to avoid backreaction postinflation. The generated magnetic field spectrum satisfies the $\gamma$-ray bound for all the possible scales of reheating. The comoving magnetic field strength and its correlation length are $\sim 4 \times 10^{-11}$ G and 70 kpc respectively, if reheating takes place at 100 GeV. For reheating at the QCD scales of 150 MeV, the field strength increases to $\sim$ nano gauss, with coherence scale of 0.6 Mpc.

DOI: 10.1103/PhysRevD.97.083503

## I. INTRODUCTION

Cosmic magnetic fields have been detected from planetary scales [1] to galaxy cluster scales [2–4]. $\gamma$-ray observations of blazars suggest their presence in the voids as well [5,6]. However, the origin of these fields does not have a fully satisfactory explanation. Astrophysical scenarios [7–11] for generating these fields involve battery effects to create a seed field which is later amplified to the observed strength by the dynamo action [12–15]. However, the presence of coherent magnetic fields in void regions favors primordial scenarios of generation. Several possible scenarios for this have been suggested in the literature [16–37] (for reviews, see [38–42]).

Inflationary magnetogenesis is one of the possible scenarios to generate fields that are coherent over large scales. However, the generation of the magnetic field during inflation in the standard physics is not possible due to the conformal invariance of the electromagnetic field [43]. A breaking of conformal invariance is necessary. This has been done in many models by taking a time dependent function coupled with the kinetic energy term of the electromagnetic (EM) field. This time dependent coupling term can arise through the coupling between inflaton field and EM field in the form $f^2F^{\mu\nu}F_{\mu\nu}$ (Ratra model) [18] or by taking a nonminimal coupling of the EM field to the gravitational field [16].

Although the Ratra model generates sufficient strength of the magnetic field, it potentially suffers from strong coupling and backreaction problems [44]. These problems have been resolved by further modification of the Ratra model [29,31,45]. In Ref. [45], to resolve these problems $f$ is assumed to increase during inflation and decrease back to its initial value post inflation. First, this behavior of $f$ circumvents the strong coupling problem. Moreover, for a small enough inflationary and reheating scales, the model also does not suffer from the backreaction problem. Indeed demanding no backreaction post inflation, bounds on the inflationary scale and reheating scale have been obtained. The generated magnetic field strength in this model can also explain the magnetic field strength suggested by $\gamma$-ray observation, below a certain reheating scale.

In the model discussed above, the generated magnetic field is of nonhelical nature. In this paper we look at the possible generation of helical magnetic fields. The nonlinear evolution of the magnetic field in the helical case differs from the nonhelical one. Due to the helicity conservation, the magnetic field strength decreases at a slower rate and the correlation length increases at a higher rate compared to the nonhelical case. Helicity conservation gives us a more optimistic evolution of the magnetic field and this can relax the bound on the reheating scale given in [45] further.

Moreover, it has been claimed in the literature that gamma ray observations of the blazars indicate the presence of the helical magnetic field in the intergalactic medium [46,47].

*rsharma@physics.du.ac.in
sharmaram.du@gmail.com
†kandu@iucaa.in
‡trs@physics.du.ac.in

 

A number of magnetogenesis scenarios have been suggested to generate helical magnetic fields. For example, such fields can be generated in models where a parity breaking term $F_{\mu\nu}\tilde{F}^{\mu\nu}$ is coupled to an axion ($\chi$) [16,48] or pseudo-Goldstone boson [49]. Here $\tilde{F}^{\mu\nu}$ is the dual electromagnetic field tensor. A hybrid of the Ratra and axion models has also been considered by adding a term $g^2F_{\mu\nu}\tilde{F}^{\mu\nu}$ to the Lagrangian of the Ratra model [30,50]. In this work, we also consider the effects of adding a similar parity breaking term. Further, we compare our generated magnetic field strength with the constraints from $\gamma$-ray observation.

This paper is organized as follows. In Sec. II we discuss the generation of the helical magnetic field during inflation. Section III discusses the generation of the field postinflation to reheating and we obtain a relation between inflationary scale and reheating scale by demanding no backreaction postinflation. Section IV incorporates the nonlinear evolution of the magnetic field and its correlation length after generation. Results of our model are also given there. In Sec. V, we compare our results with the $\gamma$-ray observation. Our conclusions are presented in Sec. VI.

## II. GENERATION OF HELICAL MAGNETIC FIELD DURING INFLATION

We start with the action for the electromagnetic field in which the conformal invariance is explicitly broken by introducing a time dependent function $f^2$ multiplying $F^{\mu\nu}F_{\mu\nu}$ in the action. To generate the helical magnetic field, we also add a $f^2F_{\mu\nu}\tilde{F}^{\mu\nu}$ in the action. Thus we take the action to be of the form

$$S = -\int \sqrt{-g}d^4x\left[\frac{f^2(\phi)}{16\pi}(F_{\mu\nu}F^{\mu\nu} + F_{\mu\nu}\tilde{F}^{\mu\nu}) + j^\mu A_\mu\right] - \int \sqrt{-g}d^4x\left[\frac{1}{2}\partial^\nu\phi\partial_\nu\phi + V(\phi)\right]. \quad (1)$$

Here $F_{\mu\nu} = \partial_\mu A_\nu - \partial_\nu A_\mu$ and $\tilde{F}^{\mu\nu} = (1/2)\epsilon^{\mu\nu\alpha\beta}F_{\alpha\beta}$, where $A_\mu$ is the EM 4-potential and $\epsilon^{\mu\nu\alpha\beta}$ is the fully antisymmetric tensor defined as $\epsilon^{\mu\nu\alpha\beta} = 1/\sqrt{-g}\eta^{\mu\nu\alpha\beta}$. $\eta^{\mu\nu\alpha\beta}$ is the Levi-Cività symbol whose values are $\pm1$ only. The term $j^\mu A_\mu$ represents the interaction where $j^\mu$ is the four current density. The remaining part of the action incorporates the evolution of the inflaton field. In this paper we adopt the following nomenclature. Greek indices $\mu, \nu\ldots$ are for space-time coordinates and Roman indices $i, j, k\ldots$ are for spatial coordinates. Our metric convention is $g_{\mu\nu} = \mathrm{diag}(-,+,+,+)$. For further analysis we assume negligible free charge density during inflation. Hence, we neglect the interaction term. To obtain the equation of motion of 4-potential $A_\mu$ we vary the action with respect to the $A_\mu$:

$$[f^2(F^{\mu\nu} + \tilde{F}^{\mu\nu})]_{;\nu} = 0$$

$$\frac{1}{\sqrt{-g}}\frac{\partial}{\partial x^\nu}\left[\sqrt{-g}f^2(\phi)\left(g^{\mu\alpha}g^{\nu\beta}F_{\alpha\beta} + \frac{1}{2\sqrt{-g}}\eta^{\mu\nu\alpha\beta}F_{\alpha\beta}\right)\right] = 0. \quad (2)$$

Varying the action with respect to the scalar field we obtain the equation governing the evolution of the scalar field as

$$\frac{1}{\sqrt{-g}}\frac{\partial}{\partial x^\nu}[\sqrt{-g}g^{\mu\nu}\partial_\mu\phi] - \frac{dV}{d\phi} = \frac{f}{2}\frac{df}{d\phi}(F_{\mu\nu}F^{\mu\nu} + F_{\mu\nu}\tilde{F}^{\mu\nu}). \quad (3)$$

Here the EM field is assumed to be a test field. Hence, it will not affect the geometry of spacetime. In the inflationary era the universe is dominated by scalar field $\phi$ which is a time dependent homogeneous field. We assume a homogeneous and isotropic universe, described by the Friedmann-Robertson-Walker line element:

$$ds^2 = -dt^2 + a^2(t)[dx^2 + dy^2 + dz^2] = a^2(\eta)[-d\eta^2 + dx^2 + dy^2 + dz^2]. \quad (4)$$

In this new coordinate system $(\eta, x, y, z)$, we can define fundamental observers with 4-velocity $(\frac{1}{a}, 0, 0, 0)$. It is convenient to work in Coulomb gauge,

$$\partial_j A^j = 0, \qquad A_0 = 0.$$

For $\mu = i$, Eq. (2) is

$$A_i'' + 2\frac{f'}{f}(A_i' + \eta_{ijk}\partial_j A_k) - a^2\partial_j\partial^j A_i = 0. \quad (5)$$

Here prime$(')$ denotes derivative with respect to $\eta$ and $\partial^j$ is defined as $\partial^j \equiv g^{jk}\partial_k = a^{-2}\delta^{jk}\partial_k$. $\eta_{ijk}$ represents the three-dimensional Levi-Cività symbol. To quantize the EM field, we calculate the conjugate momentum $(\Pi^i)$ of the $A^i$ field, promote these fields to operators and impose the canonical quantization condition,

$$\Pi^i = \frac{\delta L}{\delta \dot{A}_i}, \quad (6)$$

$$[A^i, \Pi_j] = i\int \frac{d^3k}{2\pi^3}e^{\vec{k}\cdot(\vec{x}-\vec{y})}P^i_j(k). \quad (7)$$

Here $P^i_j = \delta^i_j - \delta_{jm}(k^ik^m/k^2)$ is used to ensure the Coulomb gauge condition. We Fourier transform $A_i$ using the momentum space operators ($b_\lambda$ and $b^\dagger_\lambda$):

$$A^i(\vec{x},\eta) = \sqrt{4\pi}\int \frac{d^3k}{2\pi^3}\sum_{\lambda=1,2}\epsilon^i_\lambda[A_\lambda(k,\eta)b_\lambda(\vec{k})e^{i\vec{k}\cdot\vec{x}} + A^*_\lambda(k,\eta)b^\dagger_\lambda(\vec{k})e^{-i\vec{k}\cdot\vec{x}}]. \quad (8)$$

Here $\epsilon^i_\lambda$ represents the polarization vector which can be written in terms of the three-dimensional orthonormal unit vectors as

$$\epsilon^i_\lambda = \frac{\hat{\epsilon}^i_\lambda}{a}, \qquad \epsilon^i_3 = \frac{\hat{k}}{a}. \quad (9)$$

Here $\hat{\epsilon}^i_\lambda$ are unit 3-vectors, orthogonal to $\hat{k}$ and each other. It is useful to define a new variable $\bar{A}_\lambda$ as, $\bar{A}_\lambda = aA_\lambda(k,\eta)$. Substituting Eq. (8) in Eq. (5),

$$\sum_\lambda b_\lambda\left[\hat{\epsilon}_{i\lambda}\left(\bar{A}''_\lambda + 2\frac{f'}{f}\bar{A}'_\lambda + k^2\bar{A}_\lambda\right) + \frac{2f'}{f}\eta_{ijm}\hat{\epsilon}_{m\lambda}k_j\bar{A}_\lambda\right] = 0. \quad (10)$$

To simplify this equation further let us choose a different set of basis vectors defined as $\hat{\epsilon}_+ = (\hat{\epsilon}_1 + i\hat{\epsilon}_2)/2$ and $\hat{\epsilon}_- = (\hat{\epsilon}_1 - i\hat{\epsilon}_2)/2$. In terms of these new basis vectors, $\sum_\lambda \bar{A}_\lambda\hat{\epsilon}_\lambda b_\lambda = \bar{A}_+\hat{\epsilon}_+ b_+ + \bar{A}_-\hat{\epsilon}_- b_-$. This set of basis vectors is known as the helicity basis. Then Eq. (10) reduces to

$$\bar{A}''_h + 2\frac{f'}{f}(\bar{A}'_h + hk\bar{A}_h) + k^2\bar{A}_h = 0. \quad (11)$$

Here $h = \pm 1$ represents the helicity sign. The equation of motion in terms of $\mathcal{A}_h = f\bar{A}_h(k,\eta)$ turns out to be

$$\mathcal{A}''_h(k,\eta) + \left(k^2 - \frac{f''}{f} + 2hk\frac{f'}{f}\right)\mathcal{A}_h(k,\eta) = 0. \quad (12)$$

Before we solve the above equation for a particular $f(\phi)$, it will be of interest to calculate the energy density of the EM field. To do this we calculate the energy momentum tensor of the EM field:

$$T_{\mu\nu} \equiv -\frac{2}{\sqrt{-g}}\frac{\delta\sqrt{-g}\mathcal{L}}{\delta g^{\mu\nu}} = \frac{f^2}{4\pi}\left[g^{\alpha\beta}F_{\mu\alpha}F_{\nu\beta} - g_{\mu\nu}\frac{F^{\alpha\beta}F_{\alpha\beta}}{4}\right]. \quad (13)$$

We define the electric and magnetic field 4-vectors as $B^\mu \equiv \tilde{F}^{\mu\nu}u_\nu$ and $E^\mu \equiv F^{\mu\nu}u_\nu$. For the observer $u^\mu = (1/a,0,0,0)$, the time component of these vectors is zero. The spatial components are given by $B_i = (1/a)\eta_{ijk}\delta^{jm}\delta^{kn}\partial_m A_n$ and $E_i = -(1/a)\partial_\eta A_i$. Then the EM energy densities of ground state measured by the observer with 4-velocity $u^\mu = (1/a,0,0,0)$ are given by

$$\rho_B = \langle 0|T^B_{\mu\nu}u^\mu u^\nu|0\rangle \quad \text{and} \quad \rho_E = \langle 0|T^E_{\mu\nu}u^\mu u^\nu|0\rangle, \quad (14)$$

where we have separated the total energy density into the magnetic part and the electric part. We express these parts in terms of $A^i$ as

$$\rho_B = \langle 0|\frac{f^2}{8\pi}[\partial_i A_n\partial_j A_l(g^{ij}g^{nl} - g^{il}g^{nj})]|0\rangle = \langle 0|\frac{f^2}{8\pi}B^iB_i|0\rangle \quad (15)$$

and

$$\rho_E = \langle 0|\frac{f^2}{8\pi}[A'_iA'_jg^{ij}]|0\rangle = \langle 0|\frac{f^2}{8\pi}E^iE_i|0\rangle. \quad (16)$$

After substituting $A_i$ from Eq. (8) into Eqs. (16) and (17), and using the helicity basis, we reduce the energy densities in terms of $\mathcal{A}_+$ and $\mathcal{A}_-$:

$$\rho_B \equiv \int\frac{dk}{k}\frac{d\rho_B(k,\eta)}{d\ln k} = \int\frac{dk}{k}\frac{1}{(2\pi)^2}\frac{k^5}{a^4}(|\mathcal{A}_+(k,\eta)|^2 + |\mathcal{A}_-(k,\eta)|^2) \quad (17)$$

$$\rho_E \equiv \int\frac{dk}{k}\frac{d\rho_E(k,\eta)}{d\ln k} = \int\frac{dk}{k}\frac{f^2}{(2\pi)^2}\frac{k^3}{a^4}\left(\left|\left[\frac{\mathcal{A}_+(k,\eta)}{f}\right]'\right|^2 + \left|\left[\frac{\mathcal{A}_-(k,\eta)}{f}\right]'\right|^2\right). \quad (18)$$

In deriving the above expressions we have used the following properties:

$$b_h|0\rangle = 0 \qquad \langle 0|b_h(\vec{k})b^\dagger_{h'}(\vec{k'})|0\rangle = (2\pi)^3\delta_{hh'}\delta^3(\vec{k}-\vec{k'}).$$

In our analysis, we work with the spectral energy densities of magnetic and electric fields given by $(d\rho_B(k,\eta)/d\ln k)$ and $(d\rho_E(k,\eta)/d\ln k)$, respectively. These spectral densities represent the energy contained in the logarithmic interval in k-space.

We now turn to calculation of the magnetic and electric spectral energy densities for a particular type of coupling function. Let us assume the form of the coupling function to be a simple power law as

$$f_1(a) = f_i\left(\frac{a}{a_i}\right)^\alpha. \quad (19)$$

We assume that during inflation $f(\phi)$ has a form such that $f$ evolves with $a$ as given in (19). Here $a_i$ represents the value of the scale factor at the beginning of inflation and $\alpha$ is a real constant. By assuming the background to be purely de Sitter during inflation ($a \propto \eta^{-1}$), we get the following:

$$\frac{f_1''}{f_1} = \frac{\alpha(\alpha+1)}{\eta^2}. \tag{20}$$

For this form of coupling function Eq. (12) reduces to

$$\mathcal{A}_h''(k,\eta) + \left(k^2 - \frac{\alpha(\alpha+1)}{\eta^2} - 2hk\frac{\alpha}{\eta}\right)\mathcal{A}_h(k,\eta) = 0. \tag{21}$$

To solve Eq. (21), we rewrite it by defining some new variables, $\mu^2 \equiv \alpha(\alpha+1)+\frac{1}{4}, \kappa \equiv i\alpha h, z \equiv 2ik\eta$. Then the equation takes the form

$$\frac{\partial^2\mathcal{A}_h(k,\eta)}{\partial z^2} + \left[\frac{1}{z^2}\left(\frac{1}{4}-\mu^2\right)+\frac{\kappa}{z}-\frac{1}{4}\right]\mathcal{A}_h(k,\eta) = 0. \tag{22}$$

The solutions of this equation are Whittaker functions [51],

$$\mathcal{A}_h = c_1 W_{\kappa,\mu}(z) + c_2 W_{-\kappa,\mu}(-z). \tag{23}$$

To determine the coefficients $c_1$ and $c_2$, we have matched the solution with the bunch Davies vacuum in the subhorizon limit $|-k\eta| \gg 1$, $\mathcal{A}_h = \frac{e^{-ik\eta}}{\sqrt{2k}}$. After matching we get

$$\mathcal{A}_h = \frac{e^{\frac{i\pi\kappa}{2}}}{\sqrt{2k}} W_{\kappa,\mu}(z) = \frac{e^{\frac{-h\pi\alpha}{2}}}{\sqrt{2k}} W_{i\alpha h,\alpha+\frac{1}{2}}(2ik\eta).$$

At the end of the inflation, all the modes of cosmological interest will be outside the horizon. To get the spectral magnetic energy density of these modes, we need to write the above expression in the superhorizon limit:

$$\mathcal{A}_h = \frac{C_h}{\sqrt{2k}}[(-k\eta)^{-\alpha} + h(-k\eta)^{-\alpha+1}] + \frac{D_h}{\sqrt{2k}}\left[(-k\eta)^{1+\alpha} - \frac{h\alpha}{1+\alpha}(-k\eta)^{2+\alpha}\right]. \tag{24}$$

Here

$$C_h = e^{\frac{-h\pi\alpha}{2}}\frac{(-2i)^{-\alpha}\Gamma(1+2\alpha)}{\Gamma(1+\alpha+ih\alpha)},$$
$$D_h = e^{\frac{-h\pi\alpha}{2}}\frac{(-2i)^{1+\alpha}\Gamma(-1-2\alpha)}{\Gamma(-\alpha-ih\alpha)}. \tag{25}$$

Substituting Eq. (24) into Eq. (17) the spectral magnetic energy density comes out to be

$$\frac{d\rho_B}{d\ln k} = \frac{1}{8\pi^2}H_f^4[(|C_+|^2+|C_-|^2)(-k\eta)^{-2\alpha+4} + (|D_+|^2+|D_-|^2)(-k\eta)^{2\alpha+6}]. \tag{26}$$

Similarly the spectral electric energy density is given by

$$\frac{d\rho_E}{d\ln k} = \frac{1}{8\pi^2}H_f^4[(|C_+|^2+|C_-|^2)(-k\eta)^{-2\alpha+4} + (|D_+|^2+|D_-|^2)(1+2\alpha)^2(-k\eta)^{2\alpha+4}]. \tag{27}$$

For the expressions in Eqs. (26) and (27), we have only kept the dominant terms.

The reason for two branches in the above expressions is that $\alpha$ can be positive or negative. In the magnetic field spectrum the first branch dominates when $\alpha > 1/2$ and the other branch dominates when $\alpha < 1/2$. For the electric field spectrum the first branch dominates when $\alpha > -1/2$ and the other branch dominates when $\alpha < -1/2$. There are two possible values of $\alpha$ (namely, $\alpha = 2, -3$) for which the magnetic field spectrum is scale invariant.

For the case $\alpha = -3$, when the magnetic field is scale invariant the electric field spectrum diverges as $(-k\eta)^{-2}$. This implies that the electric field energy density may overshoot the inflaton energy density during inflation in this case and our assumption of the EM field being a test field would no longer be valid. This problem is known as the backreaction problem [44].

However, for the case $\alpha = 2$, both the magnetic and the electric field spectrum are scale invariant, and this avoids the backreaction problem. For this case the coupling function $f$ is proportional to $a^2$, which means that $f$ will be very large at the end of inflation compared to its initial value. If we assume that $f$ becomes a constant at the end of inflation, then the effective EM charge $e_f = 1/f^2$. Suppose we demand that at the end of inflation $e_f$ should have the observed value, then it will be very large at the beginning of inflation. Due to this large value of $e_f$, our perturbative analysis of field theory would no longer be valid. This problem is known as the strong coupling problem [44]. On the other hand, if $e_f$ has the observed value at the beginning of inflation, it will have a very small value at the end of inflation, avoiding the strong coupling problem. This case is further explored in the next section.

The branch $\alpha = 2$ is also preferred, as we discussed in detail in Ref. [45], because it evades the constraints imposed by the possibility of increased conductivity due to the Schwinger effect [31]. The magnetic energy spectrum at the end of inflation for $\alpha = 2$,

$$\frac{d\rho_B}{d\ln k} \approx \frac{9e^{4\pi}}{320\pi^3}H_f^4. \tag{28}$$

We note that this value is larger than the nonhelical case by a factor of $(e^{4\pi}/80\pi) \approx 10^3$.

## III. EVOLUTION AFTER INFLATION

As discussed in the last section, there are two possible scenarios for obtaining a scale invariant magnetic spectrum. The case in which $f$ is increasing during inflation avoids the backreaction problem. Moreover, if we assume that $f$

begins with a value of unity at the onset of inflation and increases during the inflationary phase, there will be no strong coupling problem. At the end of inflation, however, the EM field will be very weakly coupled to the charged particles as $f$ is much larger than unity. We address this issue in [45] by postulating that from the end of inflation onwards $f$ decreases and attains a value of unity at reheating and remains unity thereafter. This ensures that EM action is again in the standard conformally invariant form after the reheating era. Thus the deviation from the standard form is onset of inflation to the reheating.

We assume the universe to be matter dominated from the end of inflation to reheating. We consider $\alpha > 1/2$ for further analysis. In this era the evolution of the scale factor is as follows:

$$a = \frac{a_f^3 H_f^2}{4}\left(\eta + \frac{3}{a_f H_f}\right)^2$$

and the coupling function $f$ is assumed to evolve as

$$f \propto \left(\frac{a}{a_f}\right)^{-\beta}.$$

Here $a_f$ is the value of the scale factor at the end of inflation. We calculate the constant of proportionality by demanding the continuity of $f$ at the end of inflation:

$$f_2 = f_i\left(\frac{a_f}{a_i}\right)^{\alpha}\left(\frac{a}{a_f}\right)^{-\beta}.$$

To estimate the EM energy densities in this era, we need to solve Eq. (21) for this new coupling function. The solution is given by

$$\mathcal{A}_{2h} = d_1 M_{2i\beta h,-(2\beta+\frac{1}{2})}(2ik\zeta) + d_2 M_{2i\beta h,2\beta+\frac{1}{2}}(2ik\zeta). \quad (29)$$

Here $\zeta = \eta + 3/(a_f H_f)$ and $M_{2i\beta h,-(2\beta+\frac{1}{2})}(2ik\zeta)$ represents the second kind of Whittaker function [51]. To calculate $d_1$ and $d_2$, we need the above expression in the superhorizon limit. In this limit Eq. (29) becomes

$$\mathcal{A}_{2h} = d_1(2i)^{-2\beta}[(k\zeta)^{-2\beta} - h(k\zeta)^{-2\beta+1}] + d_2(2i)^{2\beta+1}\left[(k\zeta)^{2\beta+1} + \frac{2h\beta}{1+2\beta}(k\zeta)^{2\beta+2}\right]$$

and

$$\bar{A}_{2h} = \frac{\mathcal{A}_{2h}}{f_2} = \left(\frac{k}{H_f}\right)^{-2\beta}\left(d_3(1-h(k\zeta)) + d_4\left((k\zeta)^{4\beta+1} + \frac{2h\beta}{1+2\beta}(k\zeta)^{4\beta+2}\right)\right). \quad (30)$$

Here $d_3$ and $d_4$ are two new constants. They can be expressed in terms of $d_1$ and $d_2$. We demand that at the end of the inflation both $\bar{A}_h$, $\bar{A}_{2h}$ and their derivatives have to be matched. After matching we get

$$d_3 = \frac{C_h}{\sqrt{2k}}\left(\frac{k}{H_f}\right)^{-\alpha+2\beta}\left(1 + 3h\left(\frac{k}{a_f H_f}\right)\right)$$

and

$$d_4 = \frac{C_h}{\sqrt{2k}}\left(\frac{k}{H_f}\right)^{-\alpha+2\beta}\frac{3h^2}{2(4\beta+1)}\left(\frac{2k}{a_f H_f}\right)^{-4\beta+1}\left(1 - \frac{2h\beta}{1+2\beta}\frac{4\beta+2}{4\beta+1}\left(\frac{2k}{a_f H_f}\right)\right)^{-1}.$$

In $d_3$ and $d_4$ expressions, we only take the contribution of dominant terms. Energy densities after inflation evolve as

$$\frac{d\rho_B}{d\ln k} = \frac{C_1}{8\pi^2}\frac{k^4}{a^4}f_2^2(a)\left(\frac{k}{H_f}\right)^{-2\alpha}\left(1 + \frac{9}{4(4\beta+1)^2}\left(\frac{2k}{a_f H_f}\right)^{-8\beta+2}\left(\frac{2k}{aH}\right)^{8\beta+2} + \frac{3h^2}{(4\beta+1)}\left(\frac{2k}{a_f H_f}\right)^{-4\beta+1}\left(\frac{2k}{aH}\right)^{4\beta+1}\right)$$

$$\frac{d\rho_E}{d\ln k} = \frac{1}{8\pi^2}\frac{k^4}{a^4}f_2^2(a)\left(\frac{k}{H_f}\right)^{-2\alpha}\left(C_1 + \frac{9}{4}C_1\left(\frac{2k}{a_f H_f}\right)^{-8\beta+2}\left(\frac{2k}{aH}\right)^{8\beta} + 3C_2\left(\frac{2k}{a_f H_f}\right)^{-4\beta+1}\left(\frac{2k}{aH}\right)^{4\beta}\right).$$

Here $C_1 = |C_+|^2 + |C_-|^2$ and $C_2 = |C_+|^2 - |C_-|^2$. At the end of inflation, the first term inside the bracket in the expressions of $d\rho_B/d\ln k$ dominates for all the modes outside the horizon and gives a scale invariant magnetic field spectrum for $\alpha = 2$. As $f$ decreases postinflation, this term also decreases and becomes very small at reheating. Although the second and third terms are very small compared to the first term for the mode $k_i = a_i H_f$ at the end of inflation, the contribution from these terms compared to the first term increases as $f$ decreases postinflation. Consequently, the second and third terms overshoot the first term before reheating. The second term is $36/((4\beta+1)^2 a_f^4) \times (a_r/a_f)^{4\beta+1}$ times larger than the first term and $6/((4\beta+1)a_f^2) \times (a_r/a_f)^{2\beta+1/2}$ times larger than the third term at reheating for the mode which exits the horizon at the beginning of inflation ($k_i = a_i H_f$). It is even larger for all other modes of interest. After taking the contribution of the dominant term at reheating in the above expressions, we get the following expression for EM energy densities at reheating:

$$\left.\frac{d\rho_B}{d\ln k}\right|_r = \frac{9}{32\pi^2}\frac{k^4}{a_r^4}f_2^2(a_r)\left(\frac{k}{H_f}\right)^{-2\alpha}C_1\frac{1}{(4\beta+1)^2}\left(\frac{2k}{a_fH_f}\right)^{-8\beta+2}\left(\frac{2k}{a_rH_r}\right)^{8\beta+2} \tag{31}$$

$$\left.\frac{d\rho_E}{d\ln k}\right|_r = \frac{9}{32\pi^2}\frac{k^4}{a_r^4}f_2^2(a_r)\left(\frac{k}{H_f}\right)^{-2\alpha}C_1\left(\frac{2k}{a_fH_f}\right)^{-8\beta+2}\left(\frac{2k}{a_rH_r}\right)^{8\beta}. \tag{32}$$

Here $a_r$ and $H_r$ are the scale factor and Hubble parameter at reheating, respectively.

Figure 1 shows the evolution of EM and the inflaton energy densities with the scale factor, both during and after inflation. From Fig. 1 one can see that EM energy densities are increasing after inflation. It is necessary that the EM energy density does not overshoot the energy density of the universe before the coupling function $f$ reaches its preinflationary value. Since EM energy density has a monotonically increasing behavior, if $\rho_E+\rho_B<\rho_\phi$ is satisfied at reheating, it will be valid throughout the postinflationary era prior to reheating. The total EM energy density at reheating is

$$\begin{aligned}\rho_E+\rho_B|_r &= \int_{a_iH_f}^{k_r} d\ln k\left(\left.\frac{d\rho_E(k,\eta)}{d\ln k}\right|_r+\left.\frac{d\rho_B(k,\eta)}{d\ln k}\right|_r\right)\\ &= \int_{a_iH_f}^{k_r} d\ln k\left[\frac{9}{32\pi^2}\frac{k^4}{a_r^4}f_2^2(a_r)C_1\left(\frac{k}{H_f}\right)^{-2\alpha}\left(\frac{2k}{a_fH_f}\right)^{-8\beta+2}\left(\frac{2k}{a_rH_r}\right)^{8\beta}\left(1+\frac{1}{(4\beta+1)^2}\left(\frac{2k}{a_rH_r}\right)^2\right)\right]\\ &= \frac{9}{32\pi^2}\frac{f_2^2(a_r)}{a_r^4}C_1\left(\frac{k_r}{H_f}\right)^{-2\alpha}\left(\frac{2k_r}{a_fH_f}\right)^{-8\beta+2}\left(\frac{2k_r}{a_rH_r}\right)^{8\beta}k_r^4\left(\frac{1}{6-2\alpha}+\frac{1}{(8-2\alpha)(4\beta+1)^2}\left(\frac{2k_r}{a_rH_r}\right)^2\right).\end{aligned} \tag{33}$$

For further analysis we have used two new variables defined as

$$N=\ln\left(\frac{a_f}{a_i}\right) \quad \text{and} \quad N_r=\ln\left(\frac{a_r}{a_f}\right).$$

After substituting $k_r=a_rH_r=a_fH_fe^{-N_r/2}$ in Eq. (33) and using the definition of $N$ and $N_r$, we get

$$\rho_E+\rho_B|_r = C_3H_f^4e^{\alpha(2N+N_r)-7N_r}. \tag{34}$$

Here

$$C_3=\frac{9C_1}{8\pi^2}\left(\frac{1}{6-2\alpha}+\frac{4}{(8-2\alpha)(4\beta+1)^2}\right).$$

In the above expression, we also use $\beta=\alpha N/N_r$ which is obtained by demanding $f(a_r)=1$.

In order that $\rho_E+\rho_B|_r<\rho_\phi|_r$, we require

$$2\alpha(N+N_r)-(7+\alpha)N_r<\ln\left(\frac{\pi^2g_r}{30C_3}\right)-4\ln\frac{H_f}{T_r}. \tag{35}$$

Here we use $\rho_\phi|_r=g_r(\pi^2/30)T_r^4$, where $T_r$ and $g_r$ represent reheating temperature and relativistic degree of freedom, respectively, at reheating. We have several variables in the above expression but they are all not independent. To reduce the expression in terms of the minimum number of variables (independent variables), we use the following constraint.

From the isotropy of the cosmic microwave background radiation, we find the following relation:

$$N+N_r>66.9-\ln\left(\frac{T_r}{H_f}\right)-\frac{1}{3}\ln\frac{g_r}{g_0}. \tag{36}$$

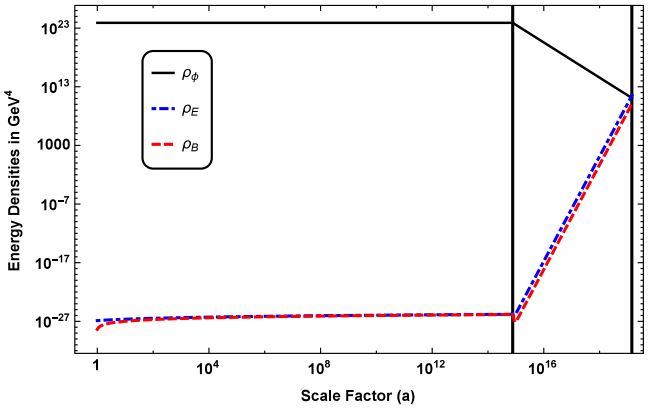


FIG. 1. In this figure we have taken $\alpha=2$ and $T_r=100$ GeV. It shows the evolution of $\rho_\phi$, $\rho_E$ and $\rho_B$ with scale factor. The first vertical bold black line is for the value of $a_f$ and the second is for the value of $a_r$. This figure shows that the energy of the EM field does not overshoot the energy of the scalar field $\phi$ which decides the background geometry if the scale of inflation and reheating satisfies the bound in Eq. (38).

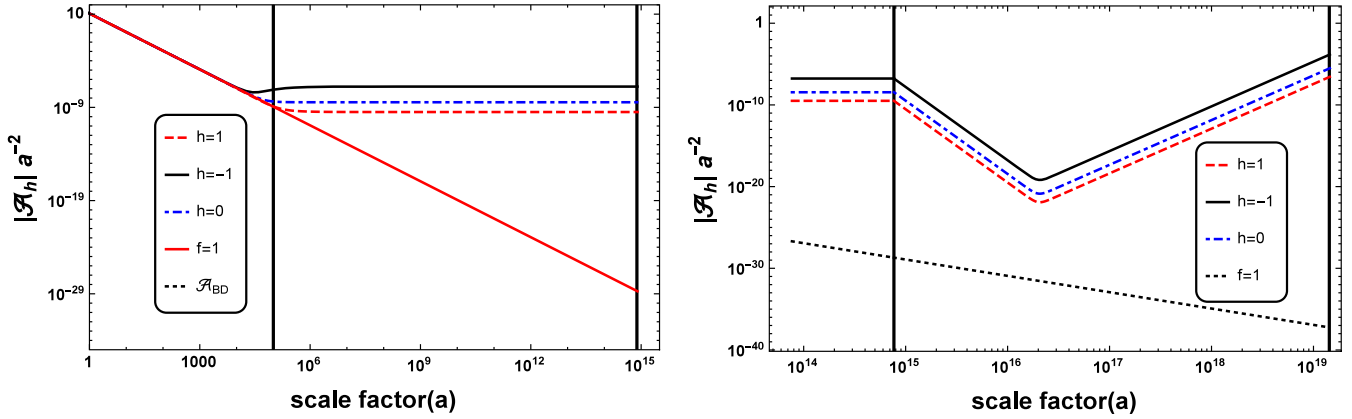


FIG. 2. In this figure we have plotted the $|\mathcal{A}_h|/a^2$ vs scale factor ($a$). Here we have assumed $\alpha = 2$, $T_r = 100$ GeV and $k = 10^5 H_f$. In the left panel, we have shown how vector potential evolves for positive helicity, negative helicity, zero helicity and for the case of constant coupling ($f = 1$) during inflation. In the second plot, we have shown the evolution of the same modes postinflation to reheating.

Here, $g_0$ is the relativistic degree of freedom in the universe at present. The above relation has been derived from the fact that the present observable universe has to be inside the Hubble radius at the beginning of inflation. In the above expression, we also assume a radiation dominated era from reheating until today.

By the assumption of matter dominance postinflation to reheating, $N_r$ can be written in terms of $H_f$ and $T_r$:

$$N_r = \frac{1}{3}\ln\frac{\rho_\phi|_{\rm inf}}{\rho_\phi|_r} = \frac{1}{3}\ln\left[\frac{90H_f^2}{8\pi G\pi^2 g_r T_r^4}\right]. \tag{37}$$

Substituting Eqs. (36) and (37) into Eq. (35) and writing $N_r$ in terms of $H_f$ and $T_r$, the bound in Eq. (35) reduces to

$$\ln\left[\frac{C_3}{g_r}\left(\frac{g_0}{g_r}\right)^{\frac{2\alpha}{3}}\left(\frac{g_r\pi^2}{30}\right)^{\frac{7+\alpha}{3}}\right] + 134\alpha + (2\alpha+4)\ln\frac{H_f}{T_r} - \frac{4(7+\alpha)}{3}\ln\left(\sqrt[4]{\frac{3H_f^2}{8\pi G}}\frac{1}{T_r}\right) < 0. \tag{38}$$

If reheating temperature and the scale of inflation satisfy the above bound, there will not be any backreaction and strong coupling problem in our prescribed model until reheating.

For further analysis, we assume a particular value of $\alpha$ and calculate the possible inflationary scales ($H_f$) for different reheating scales ($T_r$) using the bound in Eq. (38). For these $T_r$ and $H_f$, we calculate $N$ and $N_r$. We have also calculated correlation length of magnetic field and its strength at this scale at reheating using the following expressions:

$$L_c = a_r\frac{\int_0^{k_r}\frac{2\pi}{k}\frac{d\rho_B(k,\eta)}{d\ln k}d\ln k}{\int_0^{k_r}\frac{d\rho_B(k,\eta)}{d\ln k}d\ln k}$$

$$B[L_c] = \sqrt{8\pi\frac{d\rho_B(k,\eta)}{d\ln k}}\Bigg|_{k=\frac{2\pi a_r}{L_c}}. \tag{39}$$

In Fig. 2, we plot the evolution of the $|\mathcal{A}_h|/a^2$ [which appears in Eq. (17) for $\rho_B$], with scale factor for different helicity modes from the beginning of inflation to the epoch of reheating. The black solid curve and the red dotted curve show the evolution of the negative helicity and positive helicity mode, respectively. The blue dot-dashed curve shows the evolution of $|\mathcal{A}_h|/a^2$ if the parity breaking term is not present in the action (nonhelical case) and for future purpose we name this mode the zero helicity mode. If $f$ had been a constant equal to 1, the red solid curve would have represented the evolution. The black dotted curve shows the $|\mathcal{A}_h|/a^2$ for the Bunch Davies vacuum. In the left panel, the first vertical line is for the epoch of horizon crossing during inflation and the second vertical line is for the end of inflation. It is evident from the figure that negative helicity mode has a larger value than the zero helicity mode and the positive helicity mode. This means that in the helical case, the magnetic energy density is larger compared to the nonhelical case at the end of inflation and it is almost fully helical because the strength of the positive helicity mode is negligible compared to the negative helicity mode. It is also evident from this panel that without the coupling between inflaton and the EM field, the strength of the magnetic field is very small for the modes which have crossed the horizon much earlier than end of the inflation.

The right panel of Fig. 2 also follows the same color coding and it shows the postinflationary evolution until reheating. In this panel, the first vertical line is for epoch of end of inflation and the second vertical line is for the epoch of reheating. This panel shows that the strength of the mode decreases postinflation. Subsequently there is a transition and the mode starts to increase until reheating. The reason for the transition is as follows. The branch which dominated during inflation leads to both an initially dominant decaying mode and a subdominant growing mode after the transition to the matter dominated era postinflation. The

TABLE I. Present day magnetic field strength and correlation length for different reheating scales ($T_r$).

| Scale of inflation (in GeV) | Reheating temperature $T_r$ | $\alpha$ | Correlation length $L_{c0}$ (in Mpc) | Magnetic field strength $B_0[L_{c0}]$ (in G) | Correlation length $L_{c0}^{NL}$ (in Mpc) | Magnetic field strength $B_0^{NL}[L_{c0}^{NL}]$ (in G) |
|---|---|---|---|---|---|---|
| $1.14 \times 10^{10}$ | 5 MeV | 2 | $2.59 \times 10^{-5}$ | $1.60 \times 10^{-7}$ | 1.62 | $6.41 \times 10^{-9}$ |
| $2.84 \times 10^{8}$ | 150 MeV | 2 | $6.46 \times 10^{-7}$ | $9.34 \times 10^{-7}$ | 0.58 | $9.90 \times 10^{-10}$ |
| $3.88 \times 10^{5}$ | 100 GeV | 2 | $8.84 \times 10^{-10}$ | $3.43 \times 10^{-7}$ | 0.068 | $3.92 \times 10^{-11}$ |
| $3.58 \times 10^{4}$ | 1000 GeV | 2 | $8.84 \times 10^{-11}$ | $1.35 \times 10^{-7}$ | 0.032 | $7.12 \times 10^{-12}$ |

initially dominant mode decreases as $f$ decreases, while the initially subdominant one increases with time. In further evolution, naturally there is a point where both branches cross each other, this point is the transition point in the right panel. Subsequent growth of the field continues until the reheating epoch (indicated by the second vertical line). Finally on reheating the electric field gets damped by the increased plasma conductivity. The magnetic field evolves further as discussed below.

## IV. EVOLUTION OF MAGNETIC FIELD AFTER REHEATING

To determine the magnetic field strength and its correlation length at present, we need to evolve the magnetic field from the epoch of reheating to today. As we have seen in the last section, our generated magnetic field has a blue $k^4$ spectra on superhorizon scales at the time of generation. After reheating, the universe is dominated by radiation and in radiation dominance the Hubble radius increases faster than the wavelength of a mode. Due to this, modes start to reenter the horizon. As the Alfvén crossing time for a mode becomes smaller than the comoving Hubble time, nonlinear effects due to the magnetic field coupling to the plasma come into picture.

If we consider only the flux frozen evolution of the magnetic field $B \propto 1/a^2$, then magnetic field strength and its correlation length at present are given by the following expressions:

$$L_{c0} = L_c\left(\frac{a_0}{a_r}\right),$$
$$B_0[L_{c0}] = B[L_c]\left(\frac{a_0}{a_r}\right)^{-2}. \tag{40}$$

However, if we incorporate the nonlinear effects and the consequent turbulent decay of the magnetic field, its strength and correlation scale have different scaling behavior. Because of magnetic helicity conservation, inverse cascade takes place and magnetic energy transfers from smaller length scales to larger scales. This phenomenon has been discussed in [42,52,53] and also confirmed by the numerical simulations [52–57]. After using the results discussed in [42,52,53], we get the following scaling laws for the correlation scale $L_{c0}^{NL}$ and the strength of the field at this scale $B_0^{NL}[L_{c0}^{NL}]$:

$$L_{c0}^{NL} = L_{c0}\left(\frac{a_m}{a_r}\right)^{2/3},$$
$$B_0^{NL}[L_{c0}^{NL}] = B_0[L_{c0}]\left(\frac{a_m}{a_r}\right)^{-1/3}. \tag{41}$$

Here $a_m$ represents the scale factor at the matter radiation equality. As discussed in [45] there is no significant change in the comoving coherence length and field strength in the matter dominated era after $a_m$. Thus Eq. (41) gives reasonable estimates of the present day comoving field strength and correlation length. To estimate the maximum possible value of the magnetic field at different reheating scale, first we take the lowest possible scale of reheating (5 MeV) allowed by the big bang nucleosynthesis (BBN) bound [58]. We have also considered reheating scales around QCD phase transition, electroweak phase transition and at 1000 GeV. For each of these reheating temperatures we calculate the bound on the scale of inflation using Eq. (35). Further we calculate the magnetic field strength and its correlation length both assuming frozen field evolution Eq. (40) and with turbulent decay using Eq. (41). The results are given in Table I.

The bound obtained in Eq. (38) suggests that as we increase the reheating scale ($T_r$), inflationary scale ($H_f$) decreases. Since reheating occurs after the end of inflation, the above behavior suggests that the highest possible reheating scale is $\approx$4000 GeV for $\alpha = 2$. We consider several reheating scales below this highest possible reheating scale. If we consider reheating at 1000 GeV, the maximum possible magnetic field strength is $7.1 \times 10^{-12}$ G and its correlation length is 0.03 Mpc. We also calculate magnetic field strength and its correlation length for $T_r = 100$ GeV, $T_r =$ 150 MeV and $T_r = 5$ MeV and the results are shown in Table I. It is evident from the table that as we decrease the reheating temperature, the maximum possible magnetic field strength as well as its correlation length increases. Specifically, we have $B_0^{NL} \sim 3.9 \times 10^{-11}$ G, $\sim 9.9 \times 10^{-10}$ G, $6.4 \times 10^{-9}$ G for respectively $T_r = 100$ GeV, $T_r = 150$ MeV and $T_r = 5$ MeV and $L_{c0}^{NL} = 0.07$ Mpc, 0.6 Mpc and 1.6 Mpc, respectively, for the same reheating temperatures.

In the above estimates, we have assumed that the EM energy density reaches a value equal to the energy density in the inflaton field at reheating. Suppose $(\rho_E + \rho_B)|_r = \epsilon \rho_\phi|_r$, then for a particular $T_r$, the above estimated magnetic field strength will be decreased by a

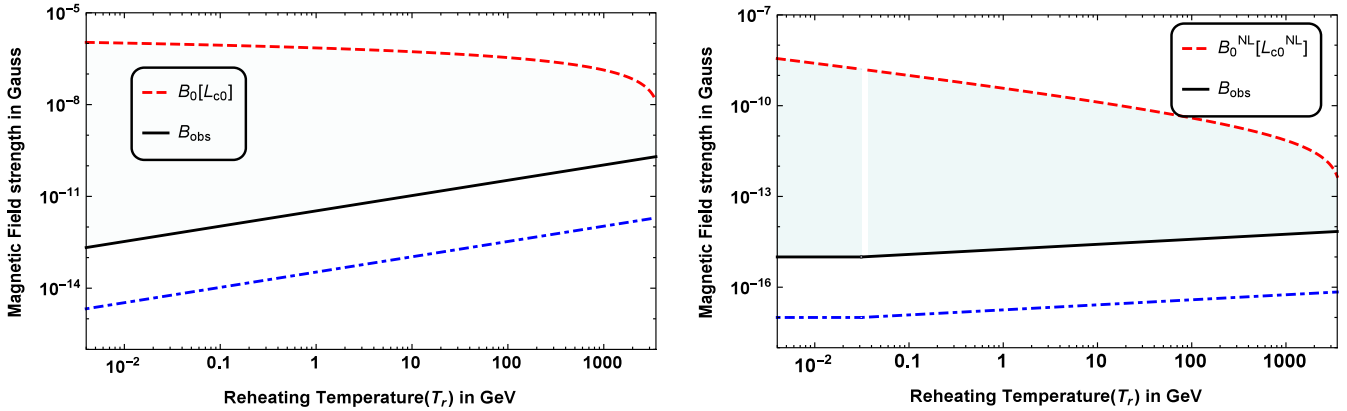


FIG. 3. We have assumed $\alpha = 2$ in plotting these figures. The black curve and dot-dashed blue curve in both parts correspond to the lower bound on observed magnetic field strength constrained by the gamma ray observations for two different mechanisms. These bounds are estimated at the correlation length of the generated magnetic field. The red dashed curve in the left panel represents the maximum magnetic field strength ($B_0[L_{c0}]$) that can be generated in our model by taking flux freezing evolution. The red dashed curve in the right panel represents the maximum magnetic field strength ($B_0^{NL}[L_{c0}^{NL}]$) that can be generated by taking the nonlinear evolution of helical magnetic fields. The shaded region in both parts represents all the allowed magnetic field strengths from $\gamma$-ray constraints.

factor of $\sqrt{\epsilon}$ but the correlation scale will remain the same. In this case, the maximum allowed value of reheating temperature is also decreased by a modest amount. For example with $\epsilon = 10^{-4}$, the maximum $T_r$ becomes ≈1300 GeV.

## V. $\gamma$-RAY CONSTRAINTS

We now consider the constraints from the $\gamma$-ray observation. Nondetection of GeV photons in blazar observation by the Fermi telescope puts a lower bound on the magnetic field strength [5,6]. Emitted photons of TeV energy from blazars interacts with the extragalactic background light and gives rise to pair production. These produced particles interact with the cosmic microwave background and generate the GeV energy photons by inverse Compton scattering. If a magnetic field is present in the intergalactic medium, it can affect the trajectories of these charge particle and observed surface brightness of GeV emission due to inverse Compton scattering can be suppressed. Further, if we consider that the size of the secondary emitting region is larger than the point spread function of the telescope then this gives a lower bound of $B \sim 10^{-15}$ G strength at the coherence scale $\geq 1$ Mpc. If the flux suppression mechanism is due to the time delay of secondary emission then one gets a lower bound of $B \sim 10^{-17}$ G at the same coherence scale. Below 1 Mpc as the coherence length decreases the lower bound on the magnetic field strength increases as $L_c^{-1/2}$ in both cases. Here $L_c$ is the comoving correlation length of the magnetic field.

In Fig. 3, we have plotted the maximum possible magnetic field strength generated in our model for different reheating scales as a dashed red curve and the two bounds on the magnetic field strength obtained from the nondetection of $\gamma$-rays from blazars respectively as a solid black curve and as a dot-dashed blue curve for the two different mechanisms. In the left panel we have only considered the flux frozen evolution of the magnetic field after generation and estimated magnetic field strength and its correlation length. In the right panel we have estimated the magnetic field strength and its correlation length by incorporating the nonlinear evolution. It is evident from the figure that the generated magnetic field strength satisfies the $\gamma$-ray observation for all possible reheating scales in our model. The shaded region in the figure represents the allowed values of magnetic fields from $\gamma$-ray observation.

In Fig. 3, we have shown the constraints only for a certain range of the reheating temperature. BBN gives us a lower bound of 5 MeV for the scale of reheating. The reason for the upper bound is discussed in the previous section. For the $\alpha = 2$ case, it is at 4000 GeV. We see from Fig. 3 that all our allowed models with $T_r < 4000$ GeV lead to magnetic fields well above the lower bound required by the $\gamma$-ray observations.

## VI. CONCLUSION

We have studied here the generation of the helical magnetic field during inflation. The generation of the magnetic field within standard physics during inflation is not possible because of the conformal invariance of the EM field. To generate magnetic field during inflation, we have adopted the Ratra model in which a coupling between the EM field and the inflaton field is assumed. We have added a parity violating term with the same coupling in our action to generate a helical magnetic field. However, this model has the well-known strong coupling and backreaction problems during inflation. We have described these problems and attempted to resolve them by adopting a particular behavior of coupling function $f$. In our model $f$ starts with a value of unity and increases during inflation so that there are no strong coupling and

backreaction problems. After inflation and before reheating it decreases such that it attains the preinflationary value at reheating to match with the observed coupling constant between the charged fields and the EM field. By demanding that there is no backreaction of the generated fields post-inflation, we get a bound on inflationary and reheating scales. For this type of evolution, the magnetic field spectrum at reheating is blue and cannot be shallower than $d\rho_b/d\ln k \propto k^4$ spectra. This spectra is obtained when $f \propto a^2$ during inflation. We have discussed this case in detail and estimate the magnetic field energy density and its correlation length for different reheating scales. If reheating happens at 100 GeV then the comoving magnetic field strength is $3.4 \times 10^{-7}$ G and its correlation length is $8.8 \times 10^{-10}$ Mpc if we only consider the flux frozen evolution. Magnetic field strength and correlation length change to $3.9 \times 10^{-11}$ G and 0.07 Mpc if we incorporate the nonlinear evolution whereby the helical field decays due to the generated magnetohydrodynamics turbulence, conserving magnetic helicity. The generated magnetic field is almost fully helical.

The generated magnetic field strength at the end of inflation is larger compared to the nonhelical case considered in Ref. [45]. Moreover, the maximum possible reheating scale in the helical case is $\approx 4 \times 10^3$ GeV which was $\approx 10^4$ GeV in the nonhelical case. We have also shown that the generated magnetic field in our model satisfies the $\gamma$-ray constraints for all the allowed reheating scales.

The behavior of coupling function which we have adopted could be obtained in hybrid inflationary scenarios [59]. In hybrid inflation, one has two scalar fields with one dominating during inflation and providing the necessary condition for inflation and other field ends the inflation. We can consider our coupling function as a function of both fields such that when the first field rolls down the potential during inflation, $f$ increases and $f$ decreases when the other field evolves.

To summarize, we have suggested a viable scenario for inflationary generation of helical magnetic fields, which does not suffer from the backreaction or strong coupling problems. In our model the generated field is almost fully helical. As we increase the reheating scale both the magnetic field strength and its correlation length decrease. However, they satisfy the $\gamma$-ray constraints for all the allowed values of reheating scales. The generated magnetic field strength and its correlation length are larger for the helical case compared to the nonhelical case. For a reheating scale at 100 GeV the magnetic field strength and its correlation length were $6.8 \times 10^{-13}$ G and $7.3 \times 10^{-4}$ Mpc for the nonhelical case [45] but $3.9 \times 10^{-11}$ G and 0.07 Mpc for the helical case. Cosmic microwave background and structure formation have mainly focused on nearly scale invariant spectra [39,42,60–67]. It would be of interest to revisit these effects for the blue spectra (see for example [68]) predicted by our consistent models of inflationary magnetogenesis.

## ACKNOWLEDGMENTS

R. S. and T. R. S. acknowledge the facilities at IUCAA Resource Center, University of Delhi, as well as the hospitality and resources provided by IUCAA, Pune, where part of this work has been done. R. S. acknowledges CSIR, India, for the financial support through Grant No. 09/045 (1343)/2014-EMR-I. T. R. S. acknowledges SERB for Project Grant No. EMR/2016/002286.

[1] D. J. Stevenson, Space Sci. Rev. **152**, 651 (2010).
[2] R. Beck, Space Sci. Rev. **99**, 243 (2001).
[3] T. E. Clarke, P. P. Kronberg, and H. Boehringer, Astrophys. J. **547**, L111 (2001).
[4] L. M. Widrow, Rev. Mod. Phys. **74**, 775 (2002).
[5] A. Neronov and I. Vovk, Science **328**, 73 (2010).
[6] A. M. Taylor, I. Vovk, and A. Neronov, Astron. Astrophys. **529**, A144 (2011).
[7] L. Biermann, Z. Naturforsch. Teil A **5**, 65 (1950).
[8] K. Subramanian, D. Narasimha, and S. M. Chitre, Mon. Not. R. Astron. Soc. **271**, L15 (1994).
[9] R. M. Kulsrud, R. Cen, J. P. Ostriker, and D. Ryu, Astrophys. J. **480**, 481 (1997).
[10] N. Y. Gnedin, A. Ferrara, and E. G. Zweibel, Astrophys. J. **539**, 505 (2000).
[11] M. J. Rees, Astron. Nachr. **327**, 395 (2006).
[12] *The Fluid Mechanics of Astrophysics and Geophysics*, Vol. 3, edited by I. B. Zeldovich, A. A. Ruzmaikin, and D. D. Sokolov (Gordon and Breach Science Publishers, New York, 1983), p. 381.
[13] A. Shukurov, in *Mathematical Aspects of Natural Dynamos*, edited by E. Dormy and A. M. Soward (Chapman & Hall/CRC, London, 2007), pp. 313–359.
[14] A. Brandenburg and K. Subramanian, Phys. Rep. **417**, 1 (2005).
[15] R. M. Kulsrud and E. G. Zweibel, Rep. Prog. Phys. **71**, 046901 (2008).
[16] M. S. Turner and L. M. Widrow, Phys. Rev. D **37**, 2743 (1988).
[17] T. Vachaspati, Phys. Lett. B **265**, 258 (1991).
[18] B. Ratra, Astrophys. J. **391**, L1 (1992).
[19] G. Sigl, A. V. Olinto, and K. Jedamzik, Phys. Rev. D **55**, 4582 (1997).
[20] L. S. Kisslinger, Phys. Rev. D **68**, 043516 (2003).
[21] Z. Berezhiani and A. D. Dolgov, Astropart. Phys. **21**, 59 (2004).

[22] K. Takahashi, K. Ichiki, H. Ohno, and H. Hanayama, Phys. Rev. Lett. **95**, 121301 (2005).
[23] R. Gopal and S. Sethi, Mon. Not. R. Astron. Soc. **363**, 521 (2005).
[24] A. G. Tevzadze, L. Kisslinger, A. Brandenburg, and T. Kahniashvili, Astrophys. J. **759**, 54 (2012).
[25] J. Martin and J. Yokoyama, J. Cosmol. Astropart. Phys. 01 (2008) 025.
[26] L. Campanelli, P. Cea, G. L. Fogli, and L. Tedesco, Phys. Rev. D **77**, 043001 (2008).
[27] R. Durrer, L. Hollenstein, and R. K. Jain, J. Cosmol. Astropart. Phys. 03 (2011) 037.
[28] I. Agullo and J. Navarro-Salas, arXiv:1309.3435.
[29] R. J. Z. Ferreira, R. K. Jain, and M. S. Sloth, J. Cosmol. Astropart. Phys. 10 (2013) 004.
[30] C. Caprini and L. Sorbo, J. Cosmol. Astropart. Phys. 10 (2014) 056.
[31] T. Kobayashi, J. Cosmol. Astropart. Phys. 14 (2014) 040.
[32] K. Atmjeet, I. Pahwa, T. R. Seshadri, and K. Subramanian, Phys. Rev. D **89**, 063002 (2014).
[33] K. Atmjeet, T. R. Seshadri, and K. Subramanian, Phys. Rev. D **91**, 103006 (2015).
[34] L. Sriramkumar, K. Atmjeet, and R. K. Jain, J. Cosmol. Astropart. Phys. 09 (2015) 010.
[35] L. Campanelli, Eur. Phys. J. C **75**, 278 (2015).
[36] G. Tasinato, J. Cosmol. Astropart. Phys. 15 (2015) 040.
[37] D. Chowdhury, L. Sriramkumar, and R. K. Jain, Phys. Rev. D **94**, 083512 (2016).
[38] D. Grasso and H. R. Rubinstein, Phys. Rep. **348**, 163 (2001).
[39] R. Durrer and A. Neronov, Astron. Astrophys. Rev. **21**, 62 (2013).
[40] K. Subramanian, Astron. Nachr. **331**, 110 (2010).
[41] A. Kandus, K. E. Kunze, and C. G. Tsagas, Phys. Rep. **505**, 1 (2011).
[42] K. Subramanian, Rep. Prog. Phys. **79**, 076901 (2016).
[43] L. Parker, Phys. Rev. Lett. **21**, 562 (1968).
[44] V. Demozzi, V. Mukhanov, and H. Rubinstein, J. Cosmol. Astropart. Phys. 08 (2009) 025.
[45] R. Sharma, S. Jagannathan, T. R. Seshadri, and K. Subramanian, Phys. Rev. D **96**, 083511 (2017).
[46] H. Tashiro, W. Chen, F. Ferrer, and T. Vachaspati, Mon. Not. R. Astron. Soc. **445**, L41 (2014).
[47] H. Tashiro and T. Vachaspati, Mon. Not. R. Astron. Soc. **448**, 299 (2015).
[48] P. Adshead, J. T. Giblin, T. R. Scully, and E. I. Sfakianakis, J. Cosmol. Astropart. Phys. 10 (2016) 039.
[49] W. D. Garretson, G. B. Field, and S. M. Carroll, Phys. Rev. D **46**, 5346 (1992).
[50] K.-W. Ng, S.-L. Cheng, and W. Lee, Chin. J. Phys. (Taipei) **53**, 110105 (2015).
[51] I. S. Gradshteyn, I. M. Ryzhik, A. Jeffrey, and D. Zwillinger, *Table of Integrals, Series, and Products*, 7th ed. (Elsevier Academic Press, New York, 2007).
[52] R. Banerjee and K. Jedamzik, Phys. Rev. D **70**, 123003 (2004).
[53] M. Christensson, M. Hindmarsh, and A. Brandenburg, Phys. Rev. E **64**, 056405 (2001).
[54] T. Kahniashvili, A. G. Tevzadze, A. Brandenburg, and A. Neronov, Phys. Rev. D **87**, 083007 (2013).
[55] T. Kahniashvili, A. Brandenburg, and A. G. Tevzadze, Phys. Scr. **91**, 104008 (2016).
[56] A. Brandenburg and T. Kahniashvili, Phys. Rev. Lett. **118**, 055102 (2017).
[57] A. Brandenburg, T. Kahniashvili, S. Mandal, A. R. Pol, A. G. Tevzadze, and T. Vachaspati, Phys. Rev. D **96**, 123528 (2017).
[58] P. F. de Salas, M. Lattanzi, G. Mangano, G. Miele, S. Pastor, and O. Pisanti, Phys. Rev. D **92**, 123534 (2015).
[59] A. Linde, Phys. Rev. D **49**, 748 (1994).
[60] S. K. Sethi and K. Subramanian, Mon. Not. R. Astron. Soc. **356**, 778 (2005).
[61] P. Trivedi, T. R. Seshadri, and K. Subramanian, Phys. Rev. Lett. **108**, 231301 (2012).
[62] P. Trivedi, K. Subramanian, and T. R. Seshadri, Phys. Rev. D **89**, 043523 (2014).
[63] P. A. R. Ade *et al.* (Planck Collaboration), Astron. Astrophys. **594**, A19 (2016).
[64] K. L. Pandey, T. R. Choudhury, S. K. Sethi, and A. Ferrara, Mon. Not. R. Astron. Soc. **451**, 1692 (2015).
[65] K. E. Kunze and E. Komatsu, J. Cosmol. Astropart. Phys. 06 (2015) 027.
[66] K. E. Kunze and M. Vzquez-Mozo, J. Cosmol. Astropart. Phys. 12 (2015) 028.
[67] J. Chluba, D. Paoletti, F. Finelli, and J.-A. Rubio-Martn, Mon. Not. R. Astron. Soc. **451**, 2244 (2015).
[68] J. M. Wagstaff and R. Banerjee, Phys. Rev. D **92**, 123004 (2015).